Approximate First-Passage Time Distributions for Gaussian Motion and Transportation Models

Marcel Reith-Braun*, Florian Pfaff*, Jakob Thumm†, and Uwe D. Hanebeck*
*Intelligent Sensor-Actuator-Systems Laboratory (ISAS)
Karlsruhe Institute of Technology (KIT), Karlsruhe, Germany
{marcel.reith-braun, pfaff, uwe.hanebeck}@kit.edu
†Cyber-Physical-Systems Group (CPS)
Technical University of Munich (TUM), Munich, Germany
jakob.thumm@tum.de

***Abstract*—We aim to approximate the distribution of the first-passage time of a particle moving according to a Gaussian process with increasing trend, i. e., the distribution of the first time a particle described, e. g., by a state-space model such as a constant-velocity or constant-acceleration model, arrives at a fixed location. Since the known approaches from the literature either consider processes from different families or lead to highly complex approximations, we seek a fast-to-compute method for the problem. Motivated by an engineering particle transport task for which we can assume that once a particle has arrived at this location it cannot move back, we derive an analytic approximation for the first-passage time probabilities and calculate its inverse cumulative distribution function analytically and the moments numerically. Furthermore, we propose a Gaussian approximation based on a linearization approach. The strengths and limitations of our methods are discussed and by comparison with Monte Carlo simulations, we show that in particular, the first one satisfies the requirements of engineering problems in terms of accuracy and computation time.**

***Index Terms*—First passage, Gaussian process, probabilistic motion model, absorbing boundary, kinematic model.**

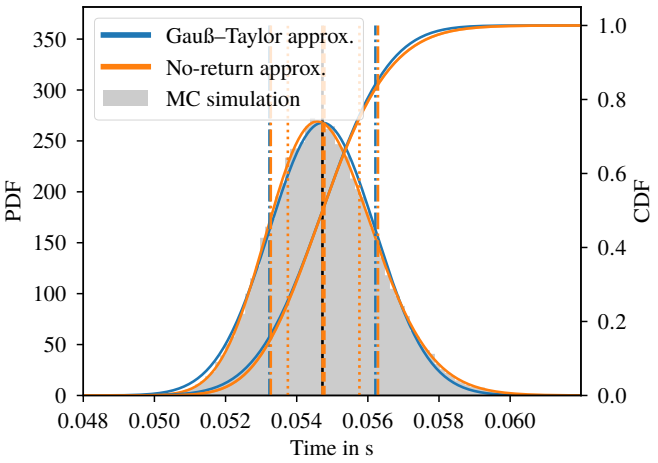

Fig. 1. Approximate first-passage time distribution and CDF for our technical transport problem using a CA model and the proposed approximation methods. Dashed-dotted vertical lines represent mean, and mean plus/minus one standard deviation. The dashed lines represent first, second, and third quantiles. The black solid vertical line illustrates the solution of the deterministic model.

I. Introduction

The problem of finding the distribution when a particle moving according to a stochastic process hits a fixed, moving, or curved boundary for the first time is called a first-passage or first-hitting time problem [1], [2]. Such problems are typically encountered in the study of diffusion processes in physics and biology but also arise, for example, in psychology, economics, signal processing, or engineering (see e. g. [3]–[5] and references therein).

In our example, we are originally motivated by the technical application of particle sorting [6], in which particles are transported by a conveyor belt while being tracked using a Kalman filter. We aim to predict the first-passage time w.r.t. an array of nozzles that is located close behind the end of the belt and ejects particles that are not of the desired class with jets of compressed air (see Fig. 2). As the filter provides us with estimated particle positions, velocities, and possibly accelerations at the end of the belt and we assume a constant velocity (CV) or constant acceleration (CA) motion model in transport direction, mathematically, this can be seen as a first-passage time problem w.r.t. a fixed boundary under stochastic initial conditions for a non-stationary, non-centered stochastic process.

Similar scenarios, where the motion of a particle or an agent is modeled by a Gaussian stochastic process with an increasing trend, i. e., an increasing mean function, are prevalent in science and engineering. One reason is that kinematic motion models perturbed by Gaussian random noise, such as CV or CA models, are still a core part of almost all applications involving state estimation or prediction. For example, such models are usually found in the field of target tracking and navigation [7], [8], autonomous driving and pedestrian motion prediction [9], or robot navigation and odometry [10]. First-passage time problems may arise there naturally, e. g., when trying to predict the time of arrival of an agent or the remaining time until a collision, where additional uncertainty information can be crucial.

Although first-passage time problems have been studied since the early 1900s, they still remain a class of challenging problems and analytic solutions are only known for some special combinations of mainly basic processes and boundaries,

e. g., Brownian motion with a fixed boundary. For general linear Gaussian state-space models (LGSSM), such as CV and CA models, no analytic solutions are known. Furthermore, the known approximation schemes for the first-passage time distribution (FPTD) and its moments are mostly designed for diffusion processes and often only available for special kinds of processes (e. g., one-dimensional, stationary, centered, or Markov). Even with the known approaches to related problems, it is our understanding that for most engineering applications, it is hard to obtain moment or quantile information within a reasonable computational time, so they do not provide a viable solution from an engineering perspective, either. Moreover, they do not take into account the characteristics typical for many motion models in engineering, such as 1) the increasing trend in the mean function and 2) the (compared with diffusion processes) generally weakly-stochastic short-time behavior. Both characteristics may allow for further approximations to achieve a good balance between approximation accuracy and computation time.

We propose two methods to tackle the problem in our engineering example: The first uses a linearization approach and assumes a Gaussian density for the FPTD whose mean and variance are calculated from the linearization. The second one exploits that particles are very unlikely to move back after passing the nozzle array, since otherwise efficient sorting would not be possible. Under this assumption, we can work with the formulas for first-passage time problems with absorbing boundaries and calculate a simple, analytic approximation for the first-passage time probabilities (see Fig. 1) without any further linearizations or assumptions on the type of distribution.

Contribution: First, we propose a simple Gaussian approximation scheme to the FPTD of LGSSMs with an increasing trend called *Gauß–Taylor approximation*. Second, we clarify the mathematical requirements that the process-boundary pair must satisfy to ensure the assumption of non-returning particles. Using this assumption, we then propose a simple analytic approximation to the FPTD called *No-return approximation* that is applicable to Gaussian processes with an increasing trend. Third, we derive the analytic solution for the corresponding quantile/percent point function (PPF) and propose a fast numerical method to obtain the moments of the approximate FPTD. We evaluate our methods for CV and CA models by comparison with Monte Carlo simulations.[1]

Notation: Vectors will be indicated by underlined letters, e. g., $\underline{x}$, and boldface capital letters, e. g., $\mathbf{A}$, will indicate matrices. We use boldface letters, $\boldsymbol{x}$, to represent random variables and time t dependencies of (random) variables, $\boldsymbol{x}(t)$, will be written in parentheses. As abbreviations, we use $\hat{x}$ for the expected value of $\boldsymbol{x}$, i. e., $\hat{x} = \mathrm{E}\{\boldsymbol{x}\}$ and the upper index t_0 to denote initial values (at time t_0), e. g., $\boldsymbol{x}^{t_0} = \boldsymbol{x}(t_0)$.

[1]Our source code is available at https://github.com/KIT-ISAS/Approx_FPTD_for_Motion_Models/tree/Fusion23

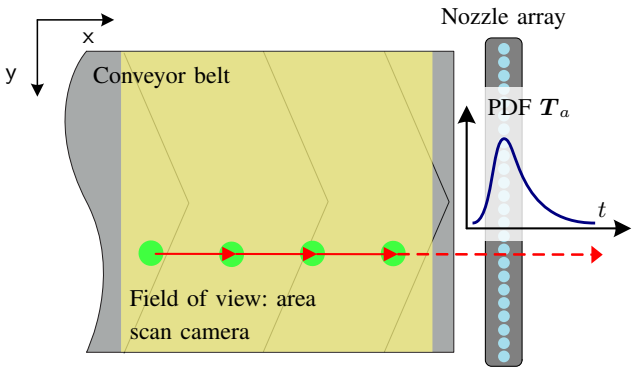

Fig. 2. Our particle sorting problem. Particles are transported to a nozzle array by a conveyor belt while being observed by an area scan camera. We assume CV or CA motion behavior and track the particles on the belt with a Kalman filter. Using the last estimated state in the camera's field of view, we aim to estimate the distribution of the particle's first-passage time $\boldsymbol{T}_a$ at the nozzle array.

II. Problem Statement

The first-passage time is defined as the first time a (continuous) random process $\boldsymbol{x}(t)$ reaches a (potentially time-dependent) value $a(t)$, i. e., $\boldsymbol{T}_a = \inf\{t > t_0 : \boldsymbol{x}(t) = a(t)\}$, when starting at a time t_0 at $\boldsymbol{x}(t_0)$ with $\boldsymbol{x}(t_0) < a(t_0)$ almost surely.[2] Our goal is to calculate the probability $\mathbb{P}(\boldsymbol{T}_a < t)$, i. e., the CDF of $\boldsymbol{T}_a$ or its PDF (the FPTD) $p_{\boldsymbol{T}_a}(t)$, if they exist. The latter requires that the first passage is an almost sure event, which might not be guaranteed for any arbitrary pairing of processes and boundaries. In this paper, we focus on fixed boundaries $a(t) = a \in \mathbb{R}$, $\forall t$ and continuous-time Gaussian processes with an increasing trend, i. e., with a continuously increasing mean function $\hat{x}(t)$ in t.

In particular, we consider time-invariant continuous-time LGSSMs without input, i. e., Markov dynamic systems that are described by the Langevin equation

$$\dot{\underline{\boldsymbol{x}}}(t) = \mathbf{A}\underline{\boldsymbol{x}}(t) + \mathbf{D}\underline{\boldsymbol{v}}(t) \ . \tag{1}$$

Here, $\underline{\boldsymbol{v}}(t)$ is a continuous, stationary, zero-mean white noise process with power spectral density $\mathbf{V}$, $\mathbf{A}$ is called the system matrix, $\mathbf{D}$ is the noise gain, and $\underline{\boldsymbol{x}}(t)$ is the state of the LGSSM. (1) has the solution

$$\underline{\boldsymbol{x}}(t) = \boldsymbol{\Phi}(t - t_0)\underline{\boldsymbol{x}}(t_0) + \int_{t_0}^{t} \boldsymbol{\Phi}(t - \tau)\mathbf{D}\underline{\boldsymbol{v}}(\tau)\,\mathrm{d}\tau \ , \tag{2}$$

where $\boldsymbol{\Phi}(\tau) = \exp(\mathbf{A}\tau)$ is the state transition matrix [7, Chapter 4]). Thus, $\underline{\boldsymbol{x}}(t)$ is given by the Gaussian process that is fully described by its mean $\hat{\underline{x}}(t) = \boldsymbol{\Phi}(t - t_0)\hat{\underline{x}}^{t_0}$, covariance

$$\boldsymbol{\Phi}(t - t_0)\boldsymbol{\Sigma}^{t_0}\boldsymbol{\Phi}^\top(t - t_0) + \int_{0}^{t-t_0} \boldsymbol{\Phi}(\tau)\mathbf{D}\mathbf{V}\mathbf{D}^\top\boldsymbol{\Phi}^\top(\tau)\,\mathrm{d}\tau \ ,$$

[2]The case where $\boldsymbol{x}(t_0) > a(t_0)$ almost surely is defined analogously.

and autocovariance $\boldsymbol{\Phi}(t-s)\mathrm{Cov}\{\underline{\boldsymbol{x}}(s)\}$, $t_0 \leq s \leq t$ with $\boldsymbol{\Sigma}^{t_0}$ the initial covariance, i. e., $\boldsymbol{\Sigma}^{t_0} = \mathrm{Cov}\{\underline{\boldsymbol{x}}(t_0)\}$ (assuming $\underline{\boldsymbol{x}}(t_0)$ to be independent of the noise) [11]. Throughout this paper, we assume w.l.o.g. that (the position) $\boldsymbol{x}(t)$ is the first component of the LGSSM's state $\underline{\boldsymbol{x}}(t)$.

Example 1 (CV Model)**.** The continuous-time CV model, also known as the white noise acceleration model, is the LGSSM with state $\underline{\boldsymbol{x}}(t) = \begin{bmatrix}\mathsf{x}(t) & \dot{\mathsf{x}}(t)\end{bmatrix}^\top$, and system matrix and noise gain

$$\mathbf{A} = \begin{bmatrix}0 & 1\\ 0 & 0\end{bmatrix}, \quad \mathbf{D} = \begin{bmatrix}0 & 1\end{bmatrix}^\top \ ,$$

where we have used $\mathsf{x}(t)$ and $\dot{\mathsf{x}}(t)$ to denote the particle's position at time t and its first temporal derivative, respectively. The system noise $\boldsymbol{v}(t)$ is therefore scalar-valued with power spectral density S. Calculation of $\boldsymbol{\Phi}(\tau)$ yields $\begin{bmatrix}1 & \tau\\ 0 & 1\end{bmatrix}$. The mean of the process evolves according to $\hat{\underline{x}}(t) = \begin{bmatrix}\hat{\mathsf{x}}^{t_0} + \hat{\dot{\mathsf{x}}}^{t_0}(t-t_0) & \hat{\dot{\mathsf{x}}}^{t_0}\end{bmatrix}^\top$ and the evolution of the covariance is given by

$$S\begin{bmatrix}\frac{(t-t_0)^3}{3} & \frac{(t-t_0)^2}{2}\\ \frac{(t-t_0)^2}{2} & t-t_0\end{bmatrix} + \begin{bmatrix}\Sigma^{t_0}_{\mathsf{x}\mathsf{x}} + 2\Sigma^{t_0}_{\mathsf{x}\dot{\mathsf{x}}}(t-t_0) + \Sigma^{t_0}_{\dot{\mathsf{x}}\dot{\mathsf{x}}}(t-t_0)^2 & \Sigma^{t_0}_{\mathsf{x}\dot{\mathsf{x}}} + \Sigma^{t_0}_{\dot{\mathsf{x}}\dot{\mathsf{x}}}(t-t_0)\\ \Sigma^{t_0}_{\mathsf{x}\dot{\mathsf{x}}} + \Sigma^{t_0}_{\dot{\mathsf{x}}\dot{\mathsf{x}}}(t-t_0) & \Sigma^{t_0}_{\dot{\mathsf{x}}\dot{\mathsf{x}}}\end{bmatrix} \ ,$$

with $\Sigma^{t_0}_{\mathsf{x}\mathsf{x}}$, $\Sigma^{t_0}_{\mathsf{x}\dot{\mathsf{x}}}$, and $\Sigma^{t_0}_{\dot{\mathsf{x}}\dot{\mathsf{x}}}$ denoting the respective entries of $\boldsymbol{\Sigma}^{t_0}$.

III. Background and Related Work

We now briefly summarize the basics of first-passage time problems and the related work for process-boundary pairs that are closest to our problem statement. For some classical results on first-passage time problems and a general review, we refer the reader to the surveys [1] and [2].

A. Background on First-Passage Times

We can find a starting point by writing the event $\{\boldsymbol{T}_a < t\}$ as the union of $\{\boldsymbol{x}(t) > a\}$ and $\{\boldsymbol{T}_a < t, \boldsymbol{x}(t) \leq a\}$, that is, to have a first-passage time $\boldsymbol{T}_a$ less than t, a particle must be located either above a at time t or, if it is below a, its path must have crossed the boundary at a time $\boldsymbol{T}_a < t$ [12]. As both events are disjoint, it follows

$$\mathbb{P}(\boldsymbol{T}_a < t) = \mathbb{P}(\boldsymbol{x}(t) > a) + \mathbb{P}(\boldsymbol{T}_a < t, \boldsymbol{x}(t) \leq a) \ . \quad (3)$$

Note that the first term on the right-hand-side of (3) is easy to compute for Gaussian processes, whereas the second term can only be computed in some special cases.

1) Method of Images: The method of images can be used to find the FPTD for Markov processes that are symmetric around the boundary [5], such as the Brownian motion $\boldsymbol{b}(t)$ with a fixed boundary. When restarting the Brownian motion at the first-passage time $\boldsymbol{T}_a$, it is equally likely that the process ends at time t below or above a, thus $\mathbb{P}(\boldsymbol{T}_a < t, \boldsymbol{b}(t) \leq a) = \mathbb{P}(\boldsymbol{T}_a < t, \boldsymbol{b}(t) > a) = \mathbb{P}(\boldsymbol{b}(t) > a)$. This is also known as the reflection principle and follows from the strong Markov property of Brownian motion (see [13], [14] for a proof). Thus,

$$\mathbb{P}(\boldsymbol{T}_a < t) = 2\mathbb{P}(\boldsymbol{b}(t) > a) = 2 - 2\Phi\left(\frac{a}{\sigma\sqrt{t}}\right) \ , \quad (4)$$

where $\Phi(\cdot)$ is the standard Gaussian CDF and σ^2 is the diffusion constant of Brownian motion. From (4), we can calculate the FPTD $p_{\boldsymbol{T}_a}(t)$ by taking the derivative w.r.t. t, which results in the Lévy distribution. Note that as $t \to \infty$, $\mathbb{P}(\boldsymbol{T}_a < t) \to 1$, which means that the first passage with an arbitrary boundary a is a sure event in case of Brownian motion.

2) Renewal Theory: For Markov processes, an integral equation can be formulated that must be satisfied by the FPTD. Let us suppose that a particular sample path crosses the border at least once between time t_0 and t, i. e., $x(t_0) \leq a \leq x(t)$. We denote the sample path's first-passage time by θ. It follows $\boldsymbol{x}(\theta) = a$. Then, due to the Markov property,

$$p(x(t)|x(t_0)) = \int_{t_0}^{t} p_{\boldsymbol{T}_a}(\theta|x(t_0))p(x(t)|x(\theta))\,\mathrm{d}\theta \ , \quad (5)$$

if $x(t) \geq a$. This integral equation is often referred to as renewal equation [1]. For some special process-boundary combinations, it is possible to solve (5) analytically (see, e. g., [1] for the Brownian motion and a fixed boundary). Since the integral of the right-hand-side of (5) is a convolution integral, (5) can be solved in Laplacian space. However, the inverse Laplace transform rarely exists, and in general, it is not possible to solve (5) for arbitrary Gauß–Markov processes. Using the Laplace transform of the renewal equation, it is, e. g., possible to find the FPTD for the Wiener process with drift $\boldsymbol{w}(t) = vt + \boldsymbol{b}(t)$, which results in the Inverse Gaussian distribution [15].

3) Absorbing Boundaries: Until now, we considered free particle motion, which means that the presence of the boundary does not affect particle motion. Opposed to that, at an absorbing boundary, a particle immediately stops moving. It thus imposes an additional boundary condition the process PDF has to fulfill (for Markov processes, one can enforce these implications when deriving the PDF via the Fokker–Planck equation). For absorbing boundary conditions and Markov processes, one can again find a renewal integral equation [3]

$$\int_{-\infty}^{a} p(x(t)|x(t_0))\,\mathrm{d}x(t) = 1 - \int_{t_0}^{t} p_{\boldsymbol{T}_a}(\theta|x(t_0))\,\mathrm{d}\theta \ . \quad (6)$$

This follows from the observation that with an absorbing boundary, the probability of not having passed the boundary by time t is equal to the probability that the first-passage time is greater than t.

B. Related Work

Here, we restrict ourselves to the related work in the field of first-passage time problems for the integrated Brownian motion $\boldsymbol{b}^{(-1)}(t) = x_0 + \int_0^t \boldsymbol{v}(\tau)\,\mathrm{d}\tau$ with $\boldsymbol{v}(t) = v_0 + \boldsymbol{b}(t)$

and deterministic initial values $\boldsymbol{x}(0) = x_0$ and $\boldsymbol{v}(0) = v_0$. This is because integrated Brownian motion is closest to LGSSMs since with the state $\underline{\boldsymbol{x}}(t) = \begin{bmatrix}\boldsymbol{b}^{(-1)}(t) & \boldsymbol{v}(t)\end{bmatrix}^\top$ one can find a state-space representation known as the Kolmogorov diffusion [16]. In particular, the CV model can be seen as a (more general) version of the integrated Brownian motion with stochastic initial conditions (note that both follow exactly the same Langevin equation and thus also the transition density and the autocovariance match). Furthermore and not restricted to integrated Brownian motion, we outline some approximation methods for estimating FPTDs.

1) Integrated Brownian Motion: Early studies on the integrated Brownian Motion with initial values $x_0 = 0$ and $v_0 > 0$ are the ones from McKean [17] and Goldman [18], who studied the first return-time to the origin. In 1985, Marshall and Watson [19] succeeded in finding the Laplace transform of the FPTD for general x_0, v_0, which allows studying the short and long-time behavior of the FPTD. However, until now, no analytic solution is known to the inverse Laplace transform. For a more comprehensive review of the relevant literature in this field, we refer the reader to the survey [20]. More recently, [21] proposed a method for finding approximate moments of the FPTD for the integrated Brownian process with $x_0 = 0$, $v_0 > 0$, $a \geq 0$ by the help of martingale methods, stopping-time arguments, and a power series approach.

2) Approximation Methods: As first-passage time problems are generally hard to solve analytically, much effort has been invested in the development of approximation methods. However, these methods are mostly designed for one-dimensional, stationary Gaussian processes. We only point out a few directions here and refer the reader to the surveys [22], [23]. One possibility is to make use of the expected number of up-crossings and express the desired probability by means of a series, often called Rice series [24]. Another approximation, especially popular in physics, is to assume that the time intervals between crossings are independent, known as the independent interval approximation (see, e. g., [5]). Another class of approximation schemes transfers the original problem to a first-passage time problem of a Wiener process with a curved boundary and approximates it by piecewise linear functions [25]. For example, [4] used this approach in combination with a series expansion to approximate the FPTD for Gauß–Markov processes.

IV. Gauss–Taylor Approximation

We now present our first approach that uses error propagation in combination with a simple Gaussian approximation for the FPTD of LGSSMs. It consists of the steps:

1) Calculate θ_d as the first-passage time of the underlying deterministic motion model, i. e., θ_d is the solution of the equation $\mathrm{E}\{\boldsymbol{x}(t)\} = a$ for t. θ_d will yield the mean of our Gaussian approximation for the FPTD.
2) Set up the motion equation

$$\underline{\boldsymbol{x}}(t) = \boldsymbol{\Phi}(t - t_0)\underline{\boldsymbol{x}}(t_0)|_{t_0=\theta_d, t=\boldsymbol{T}_a, \boldsymbol{x}(\boldsymbol{T}_a)=a}$$

at this point and solve it for $\boldsymbol{T}_a$ as a function of $\underline{\boldsymbol{x}}(\theta_d)$.
3) Linearize $\boldsymbol{T}_a(\underline{\boldsymbol{x}}(\theta_d))$ at $\mathrm{E}\{\underline{\boldsymbol{x}}(\theta_d)\}$ with a first order Taylor series expansion. This yields $\boldsymbol{T}_a(\underline{\boldsymbol{x}}(\theta_d)) \approx$

$$\boldsymbol{T}_a(\underline{\boldsymbol{x}}(\theta_d))|_{\mathrm{E}\{\underline{\boldsymbol{x}}(\theta_d)\}} + \nabla\boldsymbol{T}_a(\underline{\boldsymbol{x}}(\theta_d))|_{\mathrm{E}\{\underline{\boldsymbol{x}}(\theta_d)\}} \cdot (\underline{\boldsymbol{x}}(\theta_d) - \mathrm{E}\{\underline{\boldsymbol{x}}(\theta_d)\}) \quad .$$

4) Determine the variance of the linearization and employ it as the variance of our Gaussian approximation for the FPTD.

All steps combined result in the approximations $\mathrm{E}\{\boldsymbol{T}_a\} \approx \theta_d$ and $\mathrm{Var}\{\boldsymbol{T}_a\} = \nabla\boldsymbol{T}_a(\underline{\hat{x}}(\theta_d))^\top \mathrm{Cov}\{\underline{\boldsymbol{x}}(\theta_d)\}\nabla\boldsymbol{T}_a(\underline{\hat{x}}(\theta_d))$.

Example 1 (CV Model, continued)**.** The mean of our approximation for the CV model is given by $\theta_d = t_0 + (a - \hat{\mathrm{x}}^{t_0})/\hat{\dot{\mathrm{x}}}^{t_0}$. The motion equation in the vicinity of θ_d is

$$\boldsymbol{T}_a(\mathrm{x}(\theta_d), \dot{\mathrm{x}}(\theta_d)) = \theta_d + \frac{a - \mathrm{x}(\theta_d)}{\dot{\mathrm{x}}(\theta_d)} \quad .$$

The linearization yields $\boldsymbol{T}_a(\mathrm{x}(\theta_d), \dot{\mathrm{x}}(\theta_d)) \approx \theta_d + \frac{a-\mathrm{x}(\theta_d)}{\hat{\dot{\mathrm{x}}}(\theta_d)}$. Finally, the error propagation results in $\mathrm{Var}\{\boldsymbol{T}_a\} \approx \frac{\mathrm{Var}\{\mathrm{x}(\theta_d)\}}{\hat{\dot{\mathrm{x}}}^2(\theta_d)}$.

Note that in addition to the approximations by the Gaussian assumption and the linearization, this approach includes another approximation: When setting up the motion equation in the vicinity of θ_d, we neglect additional noise stemming from the particular solution (second term) of (2) in the time interval between θ_d and $\boldsymbol{T}_a$. Moreover, its only relation to first-passage time problems is the use of θ_d as the point of linearization.

V. No-Return Approximation

Our second proposed approximation relies on the assumption that particles are unlikely to move back once they have passed the boundary. For this, in the first part, we formalize the requirements, specify the assumption, and present our approximation. In the second part, we show how we can obtain an expression for the quantile function. Third, we propose a method for fast numerical calculation of the moments. Finally, we introduce a method for one or multidimensional Markov processes that can be used to spot-check the initial assumption.

A. Approximate First-Passage Time Probabilities

Let $\boldsymbol{x}(t)$ be a Gaussian process and $a \in \mathbb{R}$ a fixed boundary with $a > \boldsymbol{x}(t_0)$ almost surely, so that $\exists t_c \in (t_0, \infty]$ with

1) $\mathbb{P}(\boldsymbol{x}(t) > a)$ a monotonically increasing function in $[t_0, t_c]$,
2) $\mathbb{P}(\boldsymbol{x}(t_c) > a) \approx 1$, with tolerance ϵ, and
3) $\mathbb{P}(\boldsymbol{T}_a < t, \boldsymbol{x}(t) \leq a) \approx 0$, $\forall t \in [t_0, t_c)$.

The second requirement ensures that the first passage is an almost sure event since the true first-passage time probability for $t \to \infty$ is higher than $\mathbb{P}(\boldsymbol{x}(t_c) > a)$. The last point encodes our assumption that particles are unlikely to return to a level lower than a within the interval $[t_0, t_c)$. Because of the symmetry of a Gaussian process, all three requirements together can be read such that the mean is primarily responsible for the first passage.

Our approximation then is

$$\mathbb{P}(\boldsymbol{T}_a < t) \approx \begin{cases} \mathbb{P}(\boldsymbol{x}(t) > a) = \Phi\left(\frac{\mathrm{E}\{\boldsymbol{x}(t)\}-a}{\sqrt{\mathrm{Var}\{\boldsymbol{x}(t)\}}}\right) & t < t_c \\ \mathbb{P}(\boldsymbol{x}(t_c) > a) & t \geq t_c \end{cases} . \tag{7}$$

Taking the derivative with respect to t for $t < t_c$ yields an approximation for the FPTD

$$p_{T_a}(t) = \left(\frac{\frac{\mathrm{d}}{\mathrm{d}t}\mathrm{E}\{\boldsymbol{x}(t)\}}{\sqrt{\mathrm{Var}\{\boldsymbol{x}(t)\}}} + \frac{(a - \mathrm{E}\{\boldsymbol{x}(t)\})\,\frac{\mathrm{d}}{\mathrm{d}t}\mathrm{Var}\{\boldsymbol{x}(t)\}}{2\sqrt{\mathrm{Var}^3\{\boldsymbol{x}(t)\}}} \right) \frac{1}{\sqrt{2\pi}} \exp\left(-\frac{(a - \mathrm{E}\{\boldsymbol{x}(t)\})^2}{2\mathrm{Var}\{\boldsymbol{x}(t)\}} \right) . \tag{8}$$

Note that if $\mathbb{P}(\boldsymbol{x}(t) > a)$ is monotonically increasing to 1 for $t \to \infty$, the formulas describe a valid probability density. Nevertheless, if $\epsilon \neq 0$, but is small enough, we may regard (7) as a good approximation of the first-passage time CDF, although it may not reach 1 exactly and therefore is not a valid CDF in the strict sense. Note that (7) is a lower bound to the true first-passage time probability as it, according to the assumption, neglects the second term of (3) for $t < t_c$. Moreover, for $t < t_c$, (7) is essentially the same as the renewal equation for absorbing boundaries (6), and thus, the approximation can be seen as treating the boundary as an absorbing boundary, even though the stochastic process does not fulfill the implications of an absorbing boundary.

To determine t_c, we can use that $\mathbb{P}(\boldsymbol{x}(t) > a)$ has a maximum if and only if the first factor of (8) vanishes for a real $t > t_0$. Thus, one needs to solve

$$2\mathrm{Var}\{\boldsymbol{x}(t)\}\frac{\mathrm{d}}{\mathrm{d}t}\mathrm{E}\{\boldsymbol{x}(t)\} + (a - \mathrm{E}\{\boldsymbol{x}(t)\})\,\frac{\mathrm{d}}{\mathrm{d}t}\mathrm{Var}\{\boldsymbol{x}(t)\} = 0 ,$$

for $t > t_0$, which, e. g., for the CV model, is a cubic polynomial and can be solved using Cardano's formula.

While the first two requirements of our method are easy to verify, the third one needs to be examined more cautiously, since the full evaluation of $\mathbb{P}(\boldsymbol{T}_a < t, \boldsymbol{x}(t) \leq a)$ would require the true but unknown FPTD. We propose a fast method to spot-check this assumption in Sec. V-D.

B. Quantile Function

To derive the quantile function (also known as inverse CDF or PPF), we start with (7) and denote the target probability by q. Straightforward manipulations for $t < t_c$ lead to

$$\left(\Phi^{-1}(1-q)\right)^2 \mathrm{Var}\{\boldsymbol{x}(t)\} = (a - \mathrm{E}\{\boldsymbol{x}(t)\})^2 ,$$

where Φ^{-1} denotes the PPF of the standard Gaussian.

It remains to solve the equation for t. In general, this is a challenging task, as it requires solving a polynomial of degree $\max\left(d_{\mathrm{E}^2\{\boldsymbol{x}(t)\}}, d_{\mathrm{Var}\{\boldsymbol{x}(t)\}}\right)$, with $d_{\mathrm{E}^2\{\boldsymbol{x}(t)\}}$ denoting the polynomial degree of $\mathrm{E}^2\{\boldsymbol{x}(t)\}$ in t and $d_{\mathrm{Var}\{\boldsymbol{x}(t)\}}$ the polynomial degree of $\mathrm{Var}\{\boldsymbol{x}(t)\}$ in t, respectively. For some special cases, e. g., the CV model, the equation can be solved in closed form, but in general, numerical root solvers are required. For the median, i. e., $q = 0.5$, one directly obtains $a = \mathrm{E}\{\boldsymbol{x}(t)\}$. Thus, the median of our approximation corresponds to solving the process' deterministic counterpart $\mathrm{E}\{\boldsymbol{x}(t)\} = a$ for t.

C. Moments

For computing the moment of order m, in general, it is necessary to evaluate the Riemann integral $\int_{t_0}^{\infty} t^m p_{\boldsymbol{T}_a}(t)\,\mathrm{d}t$, where $p_{\boldsymbol{T}_a}(t)$ is the approximate FPTD according to (8). For the CV or CA model, this integration cannot be performed in closed form. Moreover, we have to pay attention to the integration limits, which have to be restricted to $[t_0, t_c]$ in order to avoid divergent integrals.

With these restrictions, it is possible to compute the moments numerically. For this purpose, we propose to use the CDF to accurately measure the actual probability mass in each sub-interval $[t_j, t_{j+1}]$, resulting in the approximation

$$\mathrm{E}\{\boldsymbol{T}_a^m\}_{[t_a,t_b]} \approx \sum_{j=0}^{n-1} t_j^m \left(\mathbb{P}(\boldsymbol{T}_a < t_{j+1}) - \mathbb{P}(\boldsymbol{T}_a < t_j)\right) ,$$

with integration limits $t_a, t_b \in \mathbb{R}$, integration points $t_j = t_a + j\Delta t$, $\Delta t = \frac{t_b - t_a}{n}$, and a sufficiently large $n \in \mathbb{N}$. Note that we could also approximate the moments using upper sums (t_{j+1}^m) instead of lower sums (t_j^m), and are thus directly provided with a natural measure of integration error by comparing both. It remains to find sufficient integration limits t_a and t_b. We can use the PPF to find the locations where the probability mass is located, rather than just integrating from t_0 to t_c, to construct an efficient algorithm for finding the moments.

D. Estimate of Returning Probabilities

We propose a fast-to-calculate method that indicates whether we can assume that particles are unlikely to return to the boundary after a crossing. Therefore, we calculate a time interval for which the process is highly certain to remain above the limit once it has reached it.

In the following, suppose we know the time θ of a crossing, i. e., $\boldsymbol{x}(\theta) = a$. The probability of returning below a at time $\theta + \tau$ after a crossing at time θ, $\mathbb{P}(\boldsymbol{x}(\theta + \tau) < a | \boldsymbol{x}(\theta))$, is then given by

$$\int_{-\infty}^{a} p(x(\theta + \tau)|x(\theta))\,\mathrm{d}x(\theta + \tau) . \tag{9}$$

For multivariate Markov processes, we can find an expression for $p(x(\theta + \tau)|\underline{x}(\theta))$ by writing the (full) state $\underline{\boldsymbol{x}}(\theta) = \begin{bmatrix}\boldsymbol{x}(\theta) & \underline{\boldsymbol{x}}_R(\theta)\end{bmatrix}^\top$ as a combination of the first state component $\boldsymbol{x}(\theta)$ and all remaining state components $\underline{\boldsymbol{x}}_R(\theta)$. Then, $p(x(\theta + \tau)|x(\theta))$ is given by

$$\int_{\Omega_{\underline{\boldsymbol{x}}_R(\theta+\tau)}} \int_{\Omega_{\underline{\boldsymbol{x}}_R(\theta)}} p(x(\theta + \tau), \underline{x}_R(\theta + \tau)|x(\theta), \underline{x}_R(\theta)) \cdot p(\underline{x}_R(\theta)|x(\theta))\,\mathrm{d}\underline{x}_R(\theta)\,\mathrm{d}\underline{x}_R(\theta + \tau) ,$$

where $\Omega_{\underline{\boldsymbol{x}}_R(\theta)}$ denotes the domain of $\underline{\boldsymbol{x}}_R(\theta)$. As all densities involved are Gaussians, the integration can be performed in closed form (for LGSSMs, see Appendix A).

We can now study the asymptotic behavior of $\mathbb{P}(\boldsymbol{x}(\theta+\tau) < a|\boldsymbol{x}(\theta))$. When $\lim_{\tau\to\infty} \frac{\mathrm{E}\{\boldsymbol{x}(\theta+\tau)|\boldsymbol{x}(\theta)\}-a}{\sqrt{\mathrm{Var}\{\boldsymbol{x}(\theta+\tau)|\boldsymbol{x}(\theta)\}}} = \infty$, that is, the conditional mean increases faster than the conditional standard deviation, the probability of not returning to a goes to 1. On the other hand, when $\lim_{\tau\to\infty} \frac{\mathrm{E}\{\boldsymbol{x}(\theta+\tau)|\boldsymbol{x}(\theta)\}-a}{\sqrt{\mathrm{Var}\{\boldsymbol{x}(\theta+\tau)|\boldsymbol{x}(\theta)\}}} = 0$, the probability of not returning shrinks to $\frac{1}{2}$ for $\tau \to \infty$. This implies that returning below the boundary is likely within a (small) time interval after the crossing for a process of the first class (e. g., a Wiener process with drift), whereas for the processes of the second class (e. g., a CV and CA model), the probability of returning increases when waiting long enough.

For finite τ, the probability $\mathbb{P}(\boldsymbol{x}(\theta+\tau) < a|\boldsymbol{x}(\theta))$ depends on the time θ itself. For an intuition, we could use the deterministic solution for the first-passage time θ_d, i. e., θ_d is set to the solution of $\mathrm{E}\{\boldsymbol{x}(t)\} = a$ for t. We now can again find the PPF of $\boldsymbol{x}(\theta_d+\tau) < a|\boldsymbol{x}(\theta_d)$ or use a graphical method to plot the probability over the length of the time interval. If the probability falls below a desired confidence q within a time relevant to our technical process, this is a strong indicator that condition 3) is invalid and one may consider changing the technical process or the model describing it.

Example 1 (CV Model, continued)**.** For the CV model, the process mean is given by $\mathrm{E}\{\mathsf{x}(t)\} = \hat{\mathsf{x}}^{t_0} + \hat{\dot{\mathsf{x}}}^{t_0}(t-t_0)$ and the variance by $\mathrm{Var}\{\mathsf{x}(t)\} = \Sigma_{\mathsf{xx}}^{t_0} + 2\Sigma_{\mathsf{x}\dot{\mathsf{x}}}^{t_0}(t-t_0) + \Sigma_{\dot{\mathsf{x}}\dot{\mathsf{x}}}^{t_0}(t-t_0)^2 + S\frac{(t-t_0)^3}{3}$. Thus, $\frac{\mathrm{d}}{\mathrm{d}t}\mathrm{E}\{\mathsf{x}(t)\} = \hat{\dot{\mathsf{x}}}^{t_0}$ and $\frac{\mathrm{d}}{\mathrm{d}t}\mathrm{Var}\{\mathsf{x}(t)\} = 2\Sigma_{\mathsf{x}\dot{\mathsf{x}}}^{t_0} + 2\Sigma_{\dot{\mathsf{x}}\dot{\mathsf{x}}}^{t_0}(t-t_0) + S(t-t_0)^2$. To determine t_c, one needs to solve the cubic polynomial

$$-1/3S\hat{\dot{\mathsf{x}}}^{t_0}\tilde{t}^3 + S\left(a-\hat{\mathsf{x}}^{t_0}\right)\tilde{t}^2 + 2\left(\hat{\dot{\mathsf{x}}}^{t_0}\Sigma_{\mathsf{xx}}^{t_0} + \left(a-\hat{\mathsf{x}}^{t_0}\right)\Sigma_{\mathsf{x}\dot{\mathsf{x}}}^{t_0}\right)\tilde{t} + 2\left(\hat{\dot{\mathsf{x}}}^{t_0}\Sigma_{\mathsf{xx}}^{t_0} + \left(a-\hat{\mathsf{x}}^{t_0}\right)\Sigma_{\mathsf{x}\dot{\mathsf{x}}}^{t_0}\right) = 0$$

with $\tilde{t} = t - t_0$ for t. Likewise, the calculation of the PPF results in

$$1/3Sq^2\tilde{t}^3 + \left(\Sigma_{\dot{\mathsf{x}}\dot{\mathsf{x}}}^{t_0}q^2 - \hat{\dot{\mathsf{x}}}^{t_0\,2}\right)\tilde{t}^2 + 2\left(\Sigma_{\mathsf{x}\dot{\mathsf{x}}}^{t_0}q^2 + \left(a-\hat{\mathsf{x}}^{t_0}\right)\hat{\dot{\mathsf{x}}}^{t_0}\right)\tilde{t} + \Sigma_{\mathsf{xx}}^{t_0}q^2 - \left(a-\hat{\mathsf{x}}^{t_0}\right)^2 = 0\ .$$

In particular, the median of our approximation is $t_0 + \frac{a-\hat{\mathsf{x}}^{t_0}}{\hat{\dot{\mathsf{x}}}^{t_0}}$. $p(\mathsf{x}(\theta+\tau)|\mathsf{x}(\theta))$ is given by (inserting $\mathbf{x}(\theta) = a$)

$$\mathcal{N}\Big(a + \tau\left(\hat{\dot{\mathsf{x}}}^{t_0} + \Sigma_{\dot{\mathsf{x}}\mathsf{x}}(\theta)\Sigma_{\mathsf{xx}}^{-1}(\theta)\left(a-\hat{\mathsf{x}}(\theta)\right)\right),\ \tau^2\left(\Sigma_{\dot{\mathsf{x}}\dot{\mathsf{x}}}(\theta) - \Sigma_{\mathsf{x}\dot{\mathsf{x}}}(\theta)\Sigma_{\mathsf{xx}}^{-1}(\theta)\Sigma_{\mathsf{x}\dot{\mathsf{x}}}(\theta)\right) + \frac{S}{3}\tau^3\Big)\ ,$$

with $\Sigma_{\mathsf{xx}}(\theta)$, $\Sigma_{\mathsf{x}\dot{\mathsf{x}}}(\theta)$, and $\Sigma_{\dot{\mathsf{x}}\dot{\mathsf{x}}}^{t_0}(\theta)$ denoting the respective entries of $\mathrm{Cov}\{\underline{\boldsymbol{x}}(\theta)\}$.

VI. Evaluation

We compare our two proposed approaches with Monte Carlo simulations for CV and CA models. First, we describe the properties of the processes. Second, we explain the Monte Carlo simulation. Third, we present different examples showing the strengths and limitations of the approaches.

A. Processes Used for the Evaluations

For all evaluations, we chose the following common parameters taken from a typical particle from our particle sorting application. Particles start at $\hat{\mathsf{x}}^{t_0} = 29\,\mathrm{mm}$ with velocity $\hat{\dot{\mathsf{x}}}^{t_0} = 600\,\mathrm{mm/s}$ at time $t_0 = 0$. The boundary is located at $a = 62.5\,\mathrm{mm}$. For the CA model, the acceleration is $\hat{\ddot{\mathsf{x}}}^{t_0} = 425\,\mathrm{mm/s^2}$.

B. Monte Carlo Simulations

We first discretize the continuous-time motion models with a sufficiently small time-increment Δt using the analytic solution (2) as described in [7, Chapter 6.2]. We then let each particle run until it has crossed the boundary a for the first time. Next, we compute the first-passage time using linear interpolation between the last position before and the first position after the boundary. Finally, we use histograms with 100 equally-distributed bins in the plot range to illustrate the distribution. The histograms also take into account particles that have not reached the boundary within the maximum number of time steps used, but these particles are not displayed explicitly. For all of our evaluations, we use $100\,000$ particles and a time-increment of $0.001\,\mathrm{s}$.

C. Results

The plots show the FPTDs and corresponding CDFs for our approaches. The histograms illustrate the results of the Monte Carlo approach. Vertical lines visualize the mean, variance, and the first and third quantiles of the methods, respectively. The black solid vertical lines illustrate the solutions of the deterministic model.

Fig. 3 shows the results of our method for three CV models with increasing power spectral density. For relatively low noise, i. e., for processes with a short-time behavior dominated by the mean, our methods are very close to the results of the Monte Carlo simulation. For low noise levels, the Gauß–Taylor approximation works surprisingly well. However, for higher noise levels, it fails to capture the distribution's shape correctly, while the No-return approximation still yields good results. In general, compared with the Gauß–Taylor approximation, the No-return approximation is more accurate, since it, e. g., also captures the distribution's skewness and kurtosis.

Except for the process displayed in Fig. 3c, which has an $\epsilon \approx 0.29$, all considered processes meet the requirements 1) and 2), i. e., $\mathbb{P}(\boldsymbol{x}(t) > a)$ approximately reaches 1 while increasing monotonically. For the latter process, also depicted in slightly transparent color, one can observe that $\mathbb{P}(\boldsymbol{x}(t) > a)$ decreases for $t > t_c \approx 0.104\,\mathrm{s}$. For the process in Fig. 3b, $\epsilon \approx 2 \times 10^{-8}$. For all other processes, ϵ is too small to be calculated. The same qualitative behavior as for CV models can be observed for CA models. We refer to Fig. 1 for an example with a power spectral density of $S = 9\,364\,045\,\mathrm{mm^2/s^5}$.

Fig. 4 visualizes the returning probability for $\theta = \theta_d$ for the CV model displayed in Fig. 3a. Here, to achieve a confidence of not returning higher than $95\,\%$, the time difference τ after a crossing at θ_d must be smaller than $42.58\,\mathrm{s}$. This means the technical process and its model should be such that returning

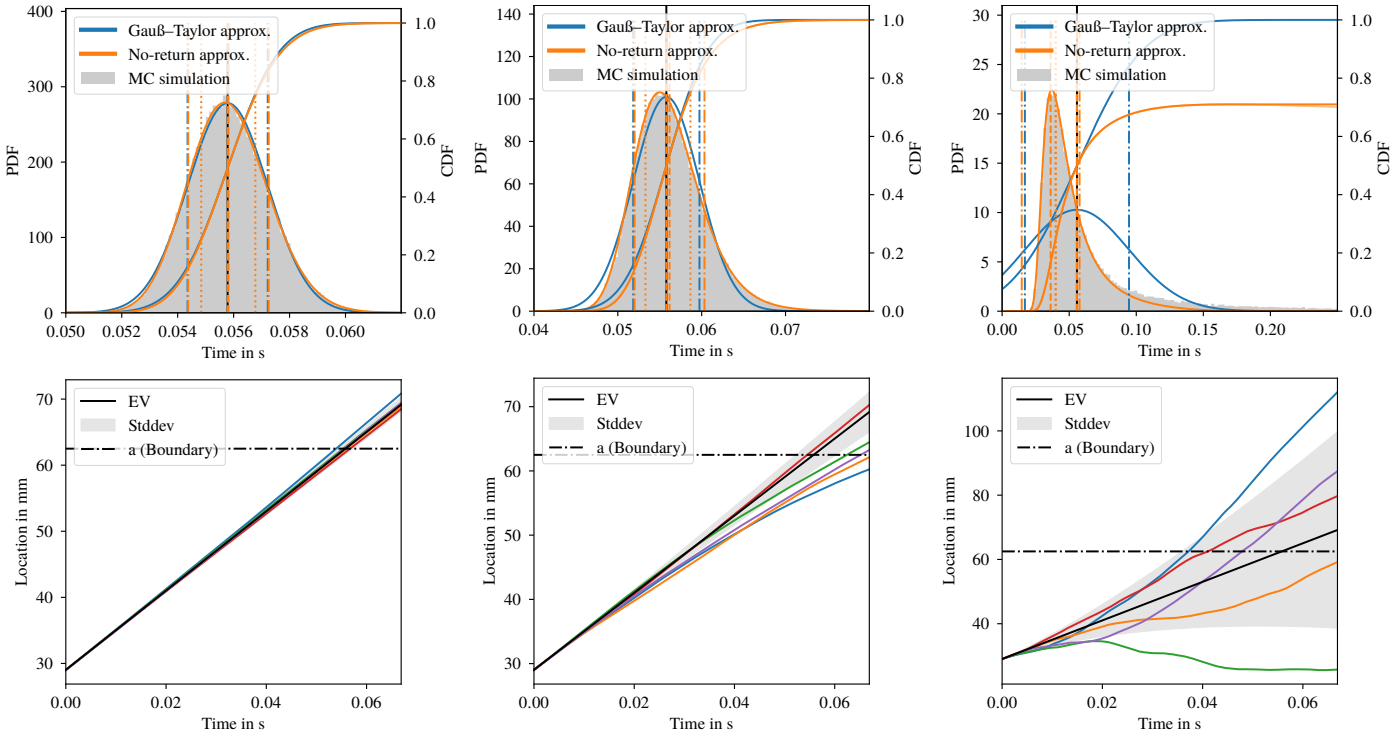

(a) $S = 9364\,\mathrm{mm^2\,s^{-3}}$ (b) $S = 93\,640\,\mathrm{mm^2\,s^{-3}}$ (c) $S = 936\,400\,\mathrm{mm^2\,s^{-3}}$

Fig. 3. FPTD (first row) and example tracks (second row) for three CV models with different power spectral densities (one per column). Dashed-dotted vertical lines in the first row represent mean, and mean plus/minus one standard deviation. The dashed lines represent first, second, and third quantiles. The plots in the second row show example tracks and the process mean (EV) and standard deviation (Stddev). The process in the first column represents a typical example of our application, the one in the middle an example with high noise, and the one in the right-hand column an artificial extreme case for which our approximations are not valid. For this process, we additionally displayed $\mathbb{P}(\boldsymbol{x}(t) > a)$ in slightly transparent color, which is visible at the right edge of the upper right plot.

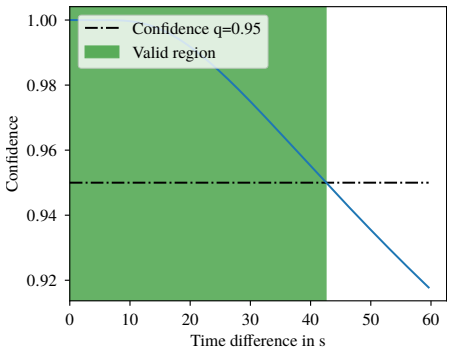

Fig. 4. Valid region of the No-return approximation for the CV model with $S = 9364\,\mathrm{mm^2/s^3}$. The green region corresponds to the time difference τ for which $\mathbb{P}(\mathbf{x}(\theta_d + \tau) > a | \mathbf{x}(\theta_d)) > 0.95$, with θ_d being the solution of the deterministic motion model.

after τ is impossible or irrelevant in order for the No-return approximation to be applicable. For the CV model with $S = 93\,640\,\mathrm{mm^2/s^3}$, τ must be smaller than $4.2\,\mathrm{s}$, and for the CV model with $S = 936\,400\,\mathrm{mm^2/s^3}$, $\tau < 0.000\,77\,\mathrm{s}$ must hold.

The calculation times of our Python implementation averaged over 10 runs are compared in Tab. I.[3] The computation times include all required operations for initializing distribution classes and calling the respective methods. The MC simulation is by far the slowest method, requiring up to about $3\,\mathrm{s}$. The Gauß–Taylor approximation performs best with calculations times up to approximately $1.2\,\mathrm{ms}$, followed by the No-return approximation with between $3.5\,\mathrm{ms}$ and $10\,\mathrm{ms}$. Note that calls to methods of already initialized classes will result in much faster calculation times.

[3]Evaluated with an Intel Core i7-6700HQ CPU, 8 × 2.60 GHz and an NVIDIA RTX 2080 Ti.

TABLE I
COMPARISON OF COMPUTATIONAL TIMES IN ms.

	MC simulation	Gauß–Taylor	No-return
PDF	2774	0.318	10.066
CDF	3153	1.156	3.53
PPF	2971	0.361	3.727
$\mathrm{E}\{\boldsymbol{T}_a\}$	2733	0.051	5.084
$\mathrm{Var}\{\boldsymbol{T}_a\}$	2774	0.056	6.129

VII. Conclusion

We proposed two methods for approximating first-passage time probabilities of Gaussian processes with an increasing trend, such as CV and CA models. The first method yields a simple Gaussian approximation by an error propagation approach. For the second method, we showed how the assumption that particles are unlikely to return to a level lower

than the boundary once they have crossed it can be used to obtain an analytic approximation for the first-passage time CDF. We then derived an expression for the PDF and its quantile function that only depends on the standard Gaussian PPF. Furthermore, we proposed a numerical method based on Riemann sums to compute the first-passage time moments. While the first approach yields reasonable results for low noise levels, empirical evaluations for the CV and the CA model prove the validity and robustness of the second method. It is thus particularly suitable for motion models from engineering, also in terms of required computation time.

Appendix A
Transition Density of LGSSMs Conditioned on One State Component

Our goal is to evaluate $p(x(\theta+\tau)|x(\theta))$

$$= \int\limits_{\Omega_{\underline{\boldsymbol{x}}_R(\theta+\tau)}} \int\limits_{\Omega_{\underline{\boldsymbol{x}}_R(\theta)}} p(x(\theta+\tau), \underline{x}_R(\theta+\tau)|x(\theta), \underline{x}_R(\theta)) \cdot p(\underline{x}_R(\theta)|x(\theta))\,\mathrm{d}\underline{x}_R(\theta)\,\mathrm{d}\underline{x}_R(\theta+\tau)\ , \tag{10}$$

where all densities involved are from an LGSSM. Furthermore, we have written the (full) state $\underline{\boldsymbol{x}}(\theta) = \begin{bmatrix}\boldsymbol{x}(\theta) & \underline{\boldsymbol{x}}_R(\theta)\end{bmatrix}^\top$ as a combination of the first state component $\boldsymbol{x}(\theta)$ and all remaining state components $\underline{\boldsymbol{x}}_R(\theta)$. Because $\underline{\boldsymbol{x}}(\theta)$ is jointly Gaussian, $p(\underline{x}_R(\theta)|x(\theta))$ is again Gaussian with mean $\mathrm{E}\{\underline{\boldsymbol{x}}_R(\theta)|\boldsymbol{x}(\theta)\} = \hat{\underline{x}}_R(\theta) + \boldsymbol{\Sigma}_{\underline{x}_R x}(\theta)\Sigma_{xx}^{-1}(\theta)\left(\boldsymbol{x}(\theta) - \hat{\mathrm{x}}(\theta)\right)$ and covariance $\mathrm{Cov}\{\underline{\boldsymbol{x}}_R(\theta)|\boldsymbol{x}(\theta)\} = \boldsymbol{\Sigma}_{\underline{x}_R\underline{x}_R}(\theta) - \boldsymbol{\Sigma}_{\underline{x}_R x}(\theta)\Sigma_{xx}^{-1}(\theta)\boldsymbol{\Sigma}_{x\underline{x}_R}(\theta)$. Here, we used $\boldsymbol{\Sigma}_{\underline{x}_R\underline{x}_R}(\theta)$, $\boldsymbol{\Sigma}_{\underline{x}_R\underline{x}_R}(\theta)$, and $\Sigma_{xx}(\theta)$ to denote the respective entries of $\mathrm{Cov}\{\underline{\boldsymbol{x}}(\theta)\}$. The LGSSM's transition density $p(\underline{x}(\theta+\tau)|\underline{x}(\theta))$ is given by the Gaussian process with mean $\boldsymbol{\Phi}(\tau)\underline{\boldsymbol{x}}(\theta)$ and covariance

$$\mathrm{Cov}\{\underline{\boldsymbol{x}}(\theta+\tau)|\underline{\boldsymbol{x}}(\theta)\} = \int\limits_0^\tau \boldsymbol{\Phi}(t)\mathbf{D}\mathbf{V}\mathbf{D}^\top\boldsymbol{\Phi}^\top(t)\,\mathrm{d}t\ .$$

Now, evaluating the inner integral of (10), incorporating that

$$\underline{\boldsymbol{x}}(\theta) = \underbrace{\begin{bmatrix}1\\0\\\vdots\\0\end{bmatrix}}_{\mathbf{S}_1\in\{0,1\}^{n_{\underline{\boldsymbol{x}}}\times 1}} \boldsymbol{x}(\theta) + \underbrace{\begin{bmatrix}0 & 0 & \dots & 0\\1 & 0 & \dots & 0\\0 & 1 & \dots & 0\\\vdots & \ddots & \ddots & \vdots\\0 & \dots & 0 & 1\end{bmatrix}}_{\mathbf{S}_2\in\{0,1\}^{n_{\underline{\boldsymbol{x}}}\times n_{\underline{\boldsymbol{x}}}-1}} \underline{\boldsymbol{x}}_R(\theta)$$

and exploiting that both processes are Gaussian, yields $p(\underline{x}(\theta+\tau)|x(\theta))$, which again is a Gaussian process with mean and covariance

$$\begin{aligned}\mathrm{E}\{\underline{\boldsymbol{x}}(\theta+\tau)|\boldsymbol{x}(\theta)\} &= \boldsymbol{\Phi}(\tau)\mathbf{S}_1\boldsymbol{x}(\theta) + \boldsymbol{\Phi}(\tau)\mathbf{S}_2\mathrm{E}\{\underline{\boldsymbol{x}}_R(\theta)|\boldsymbol{x}(\theta)\}\\ \mathrm{Cov}\{\underline{\boldsymbol{x}}(\theta+\tau)|\boldsymbol{x}(\theta)\} &= \boldsymbol{\Phi}(\tau)\mathbf{S}_2\mathrm{Cov}\{\underline{\boldsymbol{x}}_R(\theta)|\boldsymbol{x}(\theta)\}\mathbf{S}_2^\top\boldsymbol{\Phi}(\tau)^\top\\ &\quad + \mathrm{Cov}\{\underline{\boldsymbol{x}}(\theta+\tau)|\underline{\boldsymbol{x}}(\theta)\}\ .\end{aligned}$$

$p(x(\theta+\tau)|x(\theta))$ is the first component of $p(\underline{x}(\theta+\tau)|x(\theta))$.

References

[1] I. Blake and W. Lindsey, "Level-Crossing Problems for Random Processes," *IEEE Transactions on Information Theory*, vol. 19, no. 3, pp. 295–315, May 1973.

[2] A. G. Nobile *et al.*, "A Note on First-Passage Time and Some Related Problems," *Journal of Applied Probability*, vol. 22, no. 2, pp. 346–359, 1985.

[3] A. Buonocore *et al.*, "A New Integral Equation for the Evaluation of First-Passage-Time Probability Densities," *Advances in Applied Probability*, vol. 19, no. 4, pp. 784–800, 1987.

[4] E. Di Nardo *et al.*, "A Computational Approach to First-Passage-Time Problems for Gauss-Markov Processes," *Advances in Applied Probability*, vol. 33, no. 2, pp. 453–482, 2001.

[5] M. Nyberg *et al.*, "A Simple Method to Calculate First-Passage Time Densities with Arbitrary Initial Conditions," *New Journal of Physics*, vol. 18, no. 6, p. 063019, Jun. 2016.

[6] F. Pfaff, *Multitarget Tracking Using Orientation Estimation for Optical Belt Sorting*, ser. Karlsruhe Series on Intelligent Sensor-Actuator-Systems. Karlsruhe Institute of Technology, 2019, no. 22.

[7] Y. Bar-Shalom *et al.*, *Estimation with Applications to Tracking and Navigation*. John Wiley & Sons, Inc., 2001.

[8] X. R. Li and V. P. Jilkov, "Survey of Maneuvering Target Tracking. Part I. Dynamic models," *IEEE Transactions on Aerospace and Electronic Systems*, vol. 39, no. 4, pp. 1333–1364, Oct. 2003.

[9] C. Schöller *et al.*, "What the Constant Velocity Model Can Teach Us About Pedestrian Motion Prediction," *IEEE Robotics and Automation Letters*, vol. 5, no. 2, pp. 1696–1703, Apr. 2020.

[10] S. Thrun, "Probabilistic Robotics," *Communications of the ACM*, vol. 45, no. 3, pp. 52–57, Mar. 2002.

[11] P. S. Maybeck, "Chapter 4 Stochastic Processes and Linear Dynamic System Models," in *Mathematics in Science and Engineering*, ser. Stochastic models, Estimation, and Control, P. S. Maybeck, Ed. Elsevier, Jan. 1979, vol. 141, pp. 133–202.

[12] K. Lange, *Applied Probability*, ser. Springer Texts in Statistics. Springer New York, 2010.

[13] S. I. Resnick, *Adventures in Stochastic Processes*, 5th ed. Birkhauser Verlag, 1992.

[14] P. Brèmaud, *Probability Theory and Stochastic Processes*. Springer International Publishing, 2020.

[15] R. Chhikara, *The Inverse Gaussian Distribution: Theory: Methodology, and Applications*. CRC Press, 1988, vol. 95.

[16] P. Groeneboom *et al.*, "Integrated Brownian Motion, Conditioned to be Positive," *The Annals of Probability*, vol. 27, no. 3, pp. 1283 – 1303, 1999.

[17] H. P. McKean, "A Winding Problem for a Resonator Driven by a White Noise," *Journal of Mathematics of Kyoto University*, vol. 2, no. 2, pp. 227–235, 1962.

[18] M. Goldman, "On the First Passage of the Integrated Wiener Process," *Annals of Mathematical Statistics*, vol. 42, no. 6, pp. 2150–2155, 1971.

[19] T. W. Marshall and E. J. Watson, "A Drop of Ink Falls from my Pen. . . It Comes to Earth, I Know Not When," *Journal of Physics A: Mathematical and General*, vol. 18, no. 18, pp. 3531–3559, Dec. 1985.

[20] T. W. Burkhardt, "First Passage of a Randomly Accelerated Particle," in *First-passage phenomena and their applications*. World Scientific, 2014.

[21] C. H. Hesse, "On the First-Passage Time of Integrated Brownian Motion," *Journal of Applied Mathematics and Stochastic Analysis*, vol. 2005, no. 3, pp. 237–246, 2005.

[22] M. F. Kratz, "Level Crossings and other Level Functionals of Stationary Gaussian Processes," *Probability Surveys*, vol. 3, pp. 230–288, Jan. 2006.

[23] G. Lindgren, "Gaussian Integrals and Rice Series in Crossing Distributions – to Compute the Distribution of Maxima and Other Features of Gaussian Processes," *Statistical Science*, vol. 34, no. 1, pp. 100–128, Feb. 2019.

[24] J.-M. Azaïs and M. Wschebor, "The Distribution of the Maximum of a Gaussian Process: Rice Method Revisited," in *In and Out of Equilibrium*, V. Sidoravicius, Ed. Birkhäuser Boston, 2002, pp. 321–348.

[25] J. Durbin, "Boundary-Crossing Probabilities for the Brownian Motion and Poisson Processes and Techniques for Computing the Power of the Kolmogorov-Smirnov Test," *Journal of Applied Probability*, vol. 8, no. 3, pp. 431–453, 1971.